



Experimentální Analýza Napětí 2001

Experimental Stress Analysis 2001

39th International Conference

June 4 - 6, 2001 Tábor, Czech Republic

FRACTURE PROPERTIES OF HIGH STRENGTH LOW ALLOY STEELS UNDER DYNAMIC LOADING

Zdravko Praunseis^{1*}, Masao Toyoda²

Abstract:

This paper deals with an investigation of stress/strain behaviour near a notch tip under dynamic loading and its influence on the fracture property of high strength low alloy steels. Numerical finite element analysis, taking account of the strain rate effect on the flow stress, figured out that the dynamic loading elevates a local stress near the notch tip to a large extent. This was accompanied with acceleration of the strain rate on the notch tip region. Because of high-speed straining, the concentration of plastic work in the vicinity of notch tip leads to temperature rise at the notch tip. These effects contribute to fracture behaviour of materials under dynamic loading. Which effect is more dominant, stress elevation or temperature rise, depends on the toughness level of the material. For a low toughness material, the near-tip stress elevation by dynamic loading raises the ductile-brittle fracture transition temperature. By contrast, the temperature rise at the notch tip will protect the initiation of brittle fracture provided the materials holds superior fracture toughness.

Key words: HSLA steels, tensile test, finite element method, strain rate, pre-straining, dynamic loading.

1. Introduction

Deformation and fracture of structural steels and welds experienced by dynamic loading can be different significantly from those under statics conditions [1-5]. For instance, the load level necessary to yield the same amount of global deformation is apparently increased by dynamic loading. Materials may fail in a brittle manner under dynamic conditions, even though they show fully ductile behaviour under static conditions. In fact, recent two earthquakes, the Northridge and the Kobe Great Earthquakes, caused unstable fracture in steel-framed structures. The most surprising and shock event was a brittle fracture appearance of thick vertical columns at truss structures in high-rise buildings [6]. These seismic events have suggested the importance of structural redundancy to unstable fracture as well as to plastic deformation.

¹ Dr. Eng. Zdravko Praunseis, DrSc., zdravko.praunseis@uni-mb.si,

JSPS Visiting Scientist at Osaka University, Yamada-oka 2-1, Osaka 565-0871, Japan.

*University of Maribor, Faculty of Mechanical Engineering, Smetanova 17, Maribor 2000, Slovenia.

² Prof. Eng. Masao Toyoda, DrSc., toyoda@mapse.osaka-u.ac.jp,

Osaka University, Yamada-oka 2-1, Osaka 565-0871, Japan.

This paper gives an insight into strength and fracture properties of structural steels under dynamic loading. Round bar tension tests were conducted at different strain rates to understand flow properties at high-speed loading for high strength low alloy (HSLA) steels. Round-bar tension tests were conducted at different strain rates to understand flow properties at high-speed loading for HSLA steels. Attention was focused on the stress and strain fields near the notch tip. These were addressed by dynamic FE-analyses. The dynamic loading effect on the fracture behaviour of a notched tensile specimen was discussed on the basis of the characteristic near-tip stress field resulting from high-speed loading.

2. Effect of dynamic loading

It is well known that high speed straining results in an increase in yield and tensile strength, and a decrease in fracture toughness of materials. As a result, if the stress concentrator as a notch exist in a structural member, it can be supposed that the fracture transition temperature from brittle to ductile mode moves to high temperature side. The change of transition temperature is affected by the following two effects:

- a.) Stress increases under dynamic loading
- b.) Temperature increase due to high speed plastic straining, for example, about 30⁰C under 10% plastic straining condition.

The former effect can be generally evaluated by using the strain rate - temperature parameter R:

$$R = T \ln \left(A / \dot{\epsilon} \right), \quad (1)$$

where T is the temperature, $\dot{\epsilon}$ is the strain rate and A is a material constant.

By applying the above parameter r, the evaluation temperature for the required critical CTOD should change as the temperature difference ΔT_A determined by the following relation:

$$R = T_{Evaluated} \ln \left(A / \dot{\epsilon}_{Static} \right) = T_{Real} \cdot \ln \left(A / \dot{\epsilon}_{Dynamic} \right) \quad (2)$$

$$\Delta T_A = T_{Real} - T_{Evaluated} \quad (3)$$

And the second temperature increase effect due to plastic deformation also should considered for determining the evaluation temperature by considering the following equation, in which it is considered that the work by the plastic deformation converts to the temperature change:

$$\Delta T_p = \sigma \cdot \epsilon_p / (c \cdot \rho_0), \quad (4)$$

where σ : equivalent stress (MPa), ϵ_p : equivalent strain, ρ_0 : specific gravity (7.85 g/cm³),
c: specific heat (0.48 J/gK).

Consequently, the evaluating temperature with considering the dynamic straining effect is given by

$$T_{Evaluated} = T_{Real} - \Delta T_A + \Delta T_p. \quad (5)$$

3. Materials and experimental procedure

High strength low alloy HSLA steels in a quenched and tempered condition, corresponding to the grade HT 50, was used. Table 1 and Table 2 gives the chemical composition and mechanical properties of these steels. In order to compare the high strain rate effect with the pre-strain effect, both of which are important factors of seismic loading, 5 and 10% pre-strained steels were also supplied. The pre-strain was given in the rolling direction of the steel.

Table 1: Chemical composition of high strength low alloyed steel plates, grade HT 50 and 30 mm thick.

Chem. (%)	C	Si	Mn	P	S	Cr	Ni	Mo	Cu	V	Al	C_E	P_{CM}
HT 50A	0.09	0.25	0.37	0.011	0.001	0.58		0.21			0.024	0.191	0.160
HT 50B	0.06	0.40	0.90	0.015	0.001		1.10	0.33				0.158	0.170
HT 50C	0.08	0.37	0.94	0.02	0.01	0.10	0.79	0.29	0.10	0.02		0.198	0.179

Carbon equivalent C_E [7] and cold cracking parameter P_{CM} [8] is calculated as follows:

$$C_E = C + \frac{Si}{25} + \frac{Mn}{20} + \frac{Cr}{10} + \frac{Cu}{20} + \frac{Ni}{40} + \frac{Mo}{15} + \frac{V}{10} \quad (6)$$

$$P_{CM} = C + \frac{Si}{30} + \frac{Mn + Cu + Cr}{20} + \frac{Ni}{60} + \frac{Mo}{15} + \frac{V}{10} + 5B \quad (7)$$

Table 2: Mechanical properties of high strength low alloyed steel plate, grade HT 50 and 30 mm thick.

Designation	σ_Y (MPa)	σ_T (MPa)	ϵ_u (%)	CVN (J)
HT 50A	356	531	20.9	300,300,300 at -60° C
HT 50B	370	580	22	50 at -20° C
HT 50C	390	551	21.1	100 at 0° C

The round-bar specimens (Fig. 1) were extracted from middle of the plates thickness. The test in single tension were carried out for all the specimens at room temperature at strain rates in the range 10^{-4} to $10^2/s$ on 250 kN universal tension-compression machine with facilities for displacement control. During the testing, load P and the displacement over the gage length of 35.4 mm by extensometer were measured and recorded in computer. Moreover, continuous

changes in the minimum diameter of necked region or notch root and crack initiation behaviours for all types of specimens were observed and recorded by digital microscope of 25 magnifications with facilities of 13 mm depth of field.

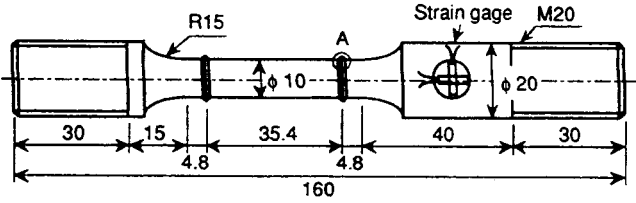


Figure 1: Geometry of round-bar specimen used for dynamic tension tests.

Yield stress and tensile strength is increased with increasing the strain rate (Fig. 2). This tendency is more appreciable in the higher strain rate region. On the other hand, the dynamic loading suppresses the work hardening property. Distinctive influence was not observed on the ductility such as the elongation and reduction area.

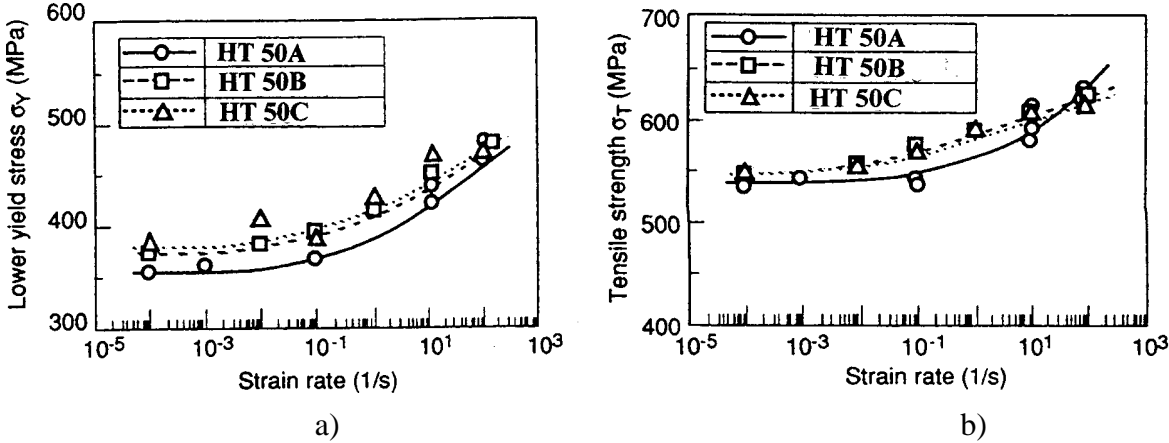


Figure 2: Effect of strain rate on yield stress (a) and tensile strength (b) of HSLA steels, grade HT 50 and 30 mm thick.

Tensile test results shown that 5% pre-strain is large enough to increase the yield stress significantly (Fig. 3). The yield stress at 5% pre-strain under static condition of 10^{-4} /s exceeds one under high-speed loading without pre-strain. The strain rate dependence for the pre-strained steels is somewhat weaker. In the case of cyclic loading, the pre-strain is accumulated during the loading history. The cyclic pre-strain has a compatible effect with the monotonic pre-strain in terms of the skeleton pre-strain, the sum of effective plastic strain produced by each load cycle. Pre-strain effect seems to be more dominant than the strain rate effect. However, the strain rate in the steel-framed structure can be accelerated to a large extent by geometrical discontinuity.

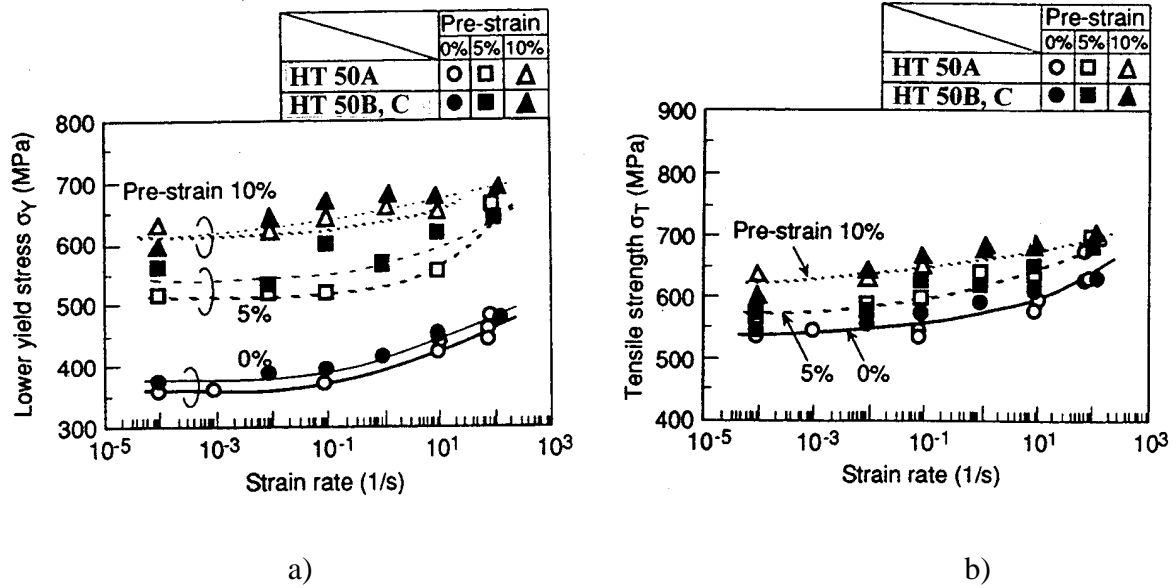


Figure 3: Comparison between strain rate effect and pre-strain effect on yield stress (a) and tensile strength (b) of HSLA steels, grade HT 50 and 30 mm thick.

5. Numerical analysis of results

The finite element (FE) analysis was conducted by using the nonlinear finite element codes, ABAQUS Ver. 5.7. Figure 4 shows the numerical model of the round-bar tensile specimen. The geometry and size is the same as those used in the tensile test. In the FE model, two dimensional axi-symmetrical element was used. Because of symmetry, the half in longitudinal direction of the specimen was modeled. Yielding condition in the FE - analysis followed von Mises yield criterion for isotropic hardening materials. The uniaxial true stress is modified by Davidenkov's equation [9] from that calculated by the current net-sectional diameter measured during the tensile test of round bar specimen.

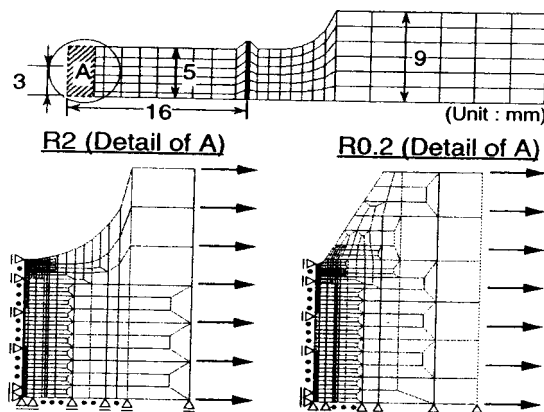


Figure 4: Mesh division of round bar tensile specimens with circumferential notch used for FE-analyses.

Figure 5 shows the analytical results of the distribution of equivalent plastic strain $\bar{\epsilon}_p$ and stress triaxiality $\sigma_m / \bar{\sigma}$ (σ_m is mean stress and $\bar{\sigma}$ is von Mises equivalent stress) in the minimum cross-section for all types of specimen at strain levels e to initiate ductile crack in each. Figure 5: Distribution of equivalent plastic strain $\bar{\epsilon}_p$ and stress triaxiality $\sigma_m / \bar{\sigma}$ in the minimum cross-section of specimens at respective strain levels e to initiate ductile crack.

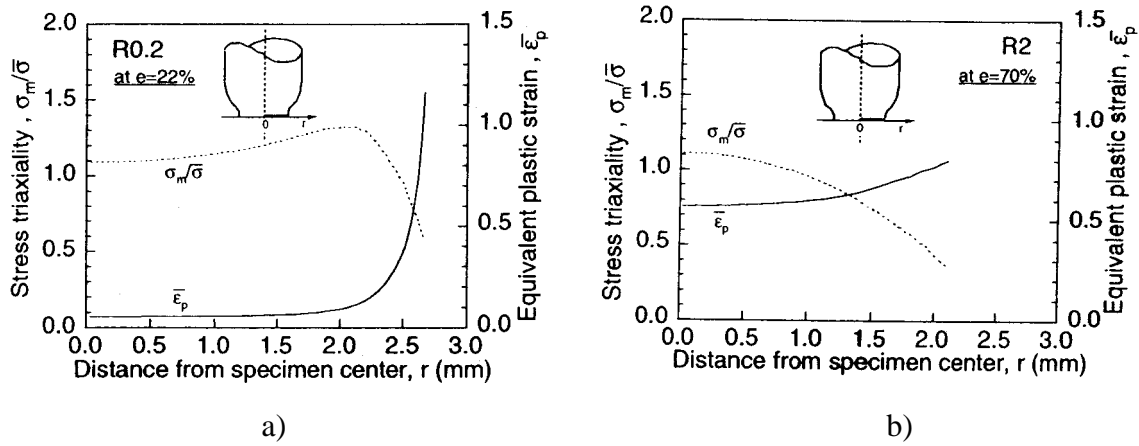


Figure 5: Distribution of equivalent plastic strain $\bar{\epsilon}_p$ and stress triaxiality $\sigma_m / \bar{\sigma}$ in the minimum cross-section of specimens R0.2 (a) and R2 (b) at respective strain levels e to initiate ductile crack.

The important to note is that in R2 specimens, in which ductile crack nucleated from the specimen center, there is almost no gradient in both $\bar{\epsilon}_p$ and $\sigma_m / \bar{\sigma}$ distributions in radial direction near the central region of net-section. On the other hand, considerable large gradient is produced near the surface of pre-notch root, from where ductile cracking occurred, in R0.2 specimens. Taking the crack initiation point observed in experiments and these stress and strain distribution into consideration, the mechanical conditions, in which the crack initiation mechanisms can operate, were considered on the basis of the two parameters criterion. Then, it was correlated the equivalent plastic strain $\bar{\epsilon}_p$ with the stress triaxiality $\sigma_m / \bar{\sigma}$ when the ductile crack occurred in the crack initiation point, these are the values in element at mid-section in R2 specimens and at the first element of pre-notch root in R0.2 specimens. Critical equivalent plastic strain required to initiate ductile crack depends largely on the stress triaxiality when the ductile crack nucleates at specimen center. Increasing of the stress triaxiality decreases the critical strain exponentially. The difference of ductile cracking controlling parameters between that from specimen center and surface could be due to the difference of the void growth modes associated with the respective stress-strain states.

6. Conclusions

Dynamic loading creates highly-activated stress fields near the notch tip compared to static loading. This is due to the evaluation of flow stress of the material by high-speed straining. The strain rate is accelerated to a large extent near the notch tip, hence the dynamic effect is more appreciable near the notch tip. Because of high-speed straining, the plastic work concentrated in the vicinity of notch tip results in temperature rise during adiabatic heating. These exclusive properties arising from high-speed straining play an important role in the

fracture behaviour of materials under dynamic conditions. For a low toughness material, the stress elevation effect is more dominant to shift the ductile-brittle fracture transition temperature to a higher temperature region. On the other hand, for the material with a superior toughness, the temperature rise effect is of advantage to reduce the transition temperature. The increase in the flow stress by high-speed straining for structural steels is described in terms of the strain rate-temperature parameter R . Under seismic loading, it is also important to consider the pre-strain effect. With the pre-strain level of 5% and the strain rate up to $10^2/s$, the pre-strain effect is more significant than the strain rate effect on the mechanical properties of HSLA steels.

Acknowledgements

One of the the authors (Z. P.) would like to take this opportunity to express his sincere gratitude to Prof. Masao Toyoda for their assistance and continuing interest in the progress of the current research. Gratitude to the Japan Society for the Promotion of Science and Slovenian Foundation of Science and Technology, Kocevar&Thermotron d.o.o, Aga Gas d.o.o and Arko d.o.o Slovenia is also noted for providing a financial support of this research program.

References

- [1] Z. Praunseis, M. P. Wnuk and M. Toyoda: "Numerical Simulation of Crack Initiation Driving Force For Strength Mis-Match Welded Joint Specimens With Surface Crack Tip In The Weld Metal", submitted to International Journal of Fracture, 2001.
- [2] Z. Praunseis: "The Influence of Microstructure on Fracture Toughness of Under-matched Weld Metal", J. Metallic Materials, Vol. 37, No. 4, pp.266 - 279, 1999.
- [3] M. Toyoda and Z. Praunseis, 2000, "The Transferability of Fracture-mechanics Parameters to Fracture Performance Evaluation of Welds with Mismatching", 8th. International Conference of Materials and Technologies in Portoroz, Slovenia, October 2000.
- [4] F. Minami and M. Toyoda: "Strength and Fracture Properties of Structural Steels", Proceedings of the 16th. International Conference on Offshore mechanics and Arctic Engineering, Editors M. Salama and M. Toyoda, 1997.
- [5] M. Ohata and M. Toyoda: "Ductile Fracture Initiation Behavior of Pipe Under a Large Scale of Cyclic Bending", Piperas Seminar, Dusseldorf, Germany, 1999.
- [6] M. Toyoda: "Brittle Fracture Controlling Factors under Seismic Loading", Proceedings of the UK-Japan Seminar, TWI, 1997.
- [7] Y. Ito and K. Bessyo: "Cracking Parameter of High Strength Steels related to Heat-Affected-Zone Cracking", Rep. 1, Jour. JWS, vol. 37, 1968, No. 9, 983-991. Rep.2, ibid, vol. 38, 1969, No. 10, 1134 -1144. IIW Doc. 1X-576-68, 1968.
- [8] C. Dueren: "Equation for the prediction of cold cracking resistance in field – welding large diameter pipes"; IX – 1356 –85.
- [9] P.W. Bridgman: "Large Plastic Flow and Fracture", McGraw-Hill, 1952.